Electronic Supplementary Material (ESI) for Polymer Chemistry.

Supporting Information

Two-dimensional single-layer supramolecular organic framework that is driven by viologen radical cation dimerization and further promoted by cucurbit[8]uril

Liang Zhang,[a] Tian-You Zhou,[b] Jia Tian,[a] Hui Wang,[a] Dan-Wei Zhang,[a] Xin Zhao,[b] Yi Liu,[c]* and Zhan-Ting Li[a]**

[a]*Department of Chemistry, Fudan University, 220 Handan Road, Shanghai 200433, China*

[b]*Shanghai Institute of Organic Chemistry, Chinese Academy of Sciences, 345 Lingling Lu, Shanghai 200032, China*

[c]*The Molecular Foundry, Lawrence Berkeley National Laboratory, One Cyclotron Road, Berkeley, CA 94720, USA*

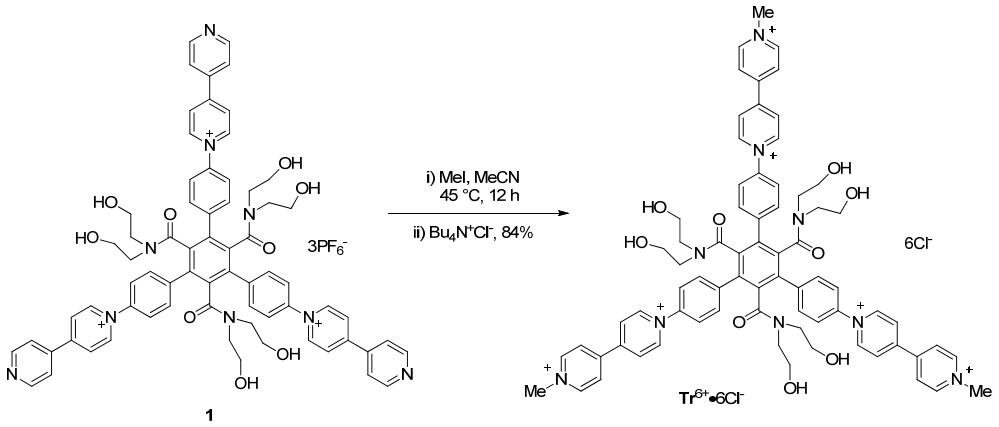

Compound Tr^{6+}·6Cl⁻. A solution of compound **1**[1] (0.19 g, 0.12 mmol) and methyl iodide (0.36 g, 2.50 mmol) in acetonitrile was stirred at 45 °C for 12 h and then was added tetrabutylammonium chloride (2.78 g, 10.0 mmol). The solution was cooled to room temperature and the formed solid was filtrated and washed with acetonitrile (100 mL). The crude product was further recrystallized from methanol and THF to give compound $\mathbf{Tr}^{6+}$·6Cl⁻ as a yellow solid (0.17 g, 84 %). M.p. >300 °C. ^{1}H NMR (400 MHz, D_2O): δ 9.40 (d, J = 4.0 Hz, 6H), 9.08 (d, J = 8.0 Hz, 6H), 8.74 (d, J = 4.0 Hz, 6H), 8.60 (d, J = 8.0 Hz, 6H), 8.11-7.88 (m, 12H), 4.52-4.49 (m, 9H), 3.71-3.05 (m, 24H). ^{13}C NMR (100 MHz, D_2O): δ 169.2, 168.7, 151.4, 149.5, 146.4, 145.4, 143.0, 138.0, 136.5, 135.2, 127.2, 126.9, 124.2, 124.1, 58.3, 58.2, 57.6, 57.5, 51.7, 51.3, 48.4, 45.9, 45.8. HRMS (ESI): calcd for $C_{72}H_{75}F_{18}N_9O_9P_3$ $[M\text{-}3PF_6]^{3+}$: 548.1532, found: 548.1530; calcd for $C_{72}H_{75}F_{12}N_9O_9P_2$ $[M\text{-}2PF_6]^{4+}$: 374.8737, found: 374.8730; calcd for $C_{72}H_{75}N_9O_9$ $[M]^{6+}$: 201.5943, found: 201.5942.

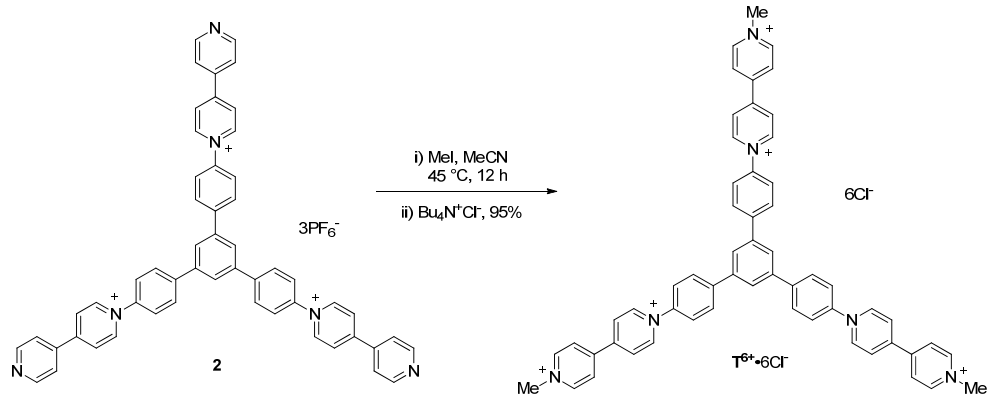

Compound T^{6+}·6Cl⁻. A solution of compound **2**[1] (0.12 g, 0.1 mmol) and methyl iodide (0.36 g, 2.50 mmol) in acetonitrile was stirred at 45 °C for 12 h and then was added tetrabutylammonium chloride (2.78 g, 10.0 mmol). The solution was cooled to room temperature and the formed solid was filtrated. The solid was washed with acetonitrile (50 mL) and dried in vacuo to give compound $\mathbf{T}^{6+}$·6Cl⁻ as a yellow solid (0.10 g, 95%). M.p. >300 °C. ^{1}H NMR (400 MHz, D_2O): δ 9.36 (d, J = 8.0 Hz, 6H), 8.98 (d, J = 4.0 Hz, 6H), 8.64 (d, J = 8.0 Hz, 6H), 8.51 (d, J = 4.0 Hz, 6H), 8.14 (s, 3H), 8.10 (d, J = 8.0 Hz, 6H), 7.89 (d, J = 8.0 Hz, 6H), 4.41 (s, 9H). ^{13}C NMR (100 MHz, D_2O): δ146.4, 145.4, 129.4, 127.1, 126.8, 126.7, 124.7, 68.3. HRMS (ESI): calcd for $C_{57}H_{48}N_6$ $[M]^{6+}$: 136.0651, found: 136.0648.

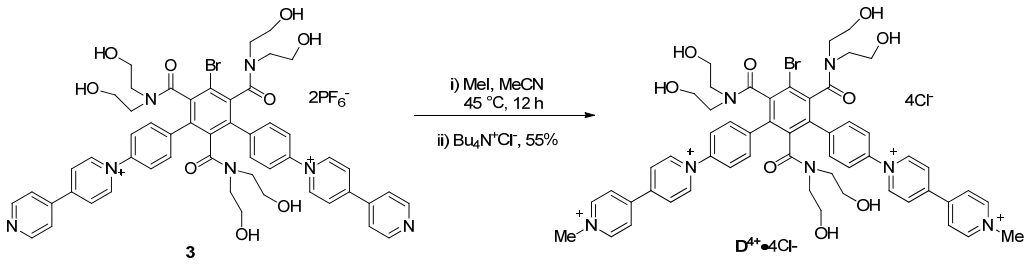

Compound D^{4+}·4Cl⁻. A solution of compound **3**[1] (0.26 g, 0.2 mmol) and methyl iodide (0.36 g, 2.50 mmol) in acetonitrile was stirred at 45 °C for 12 h and then was added tetrabutylammonium chloride (2.78 g, 10.0 mmol). The solution was cooled to room temperature and the formed solid was filtrated and washed with acetonitrile (100 mL). The crude product was further recrystallized from methanol and THF to give compound $\mathbf{D}^{4+}$·4Cl⁻. as a yellow solid (0.13 g, 55 %). M.p. >300 °C. ^{1}H NMR (400 MHz, D_2O): δ 9.44 (d, *J* = 8.0 Hz, 4H), 9.11 (d, *J* = 8.0 Hz, 4H), 8.78 (d, *J* = 8.0 Hz, 4H), 8.63 (d, *J* = 4.0 Hz, 4H), 8.21-7.82 (m, 8H), 4.54 (s, 6H), 3.81-3.13 (m, 23H) 2.81-2.72 (m, 1H). ^{13}C NMR (100 MHz, D_2O): δ 168.8, 151.3, 149.5, 146.4, 145.5, 143.3, 143.1, 142.9, 138.2, 137.4, 136.1, 135.6, 132.3, 127.3, 126.9, 124.8, 124.4, 119.1, 118.6, 58.5, 58.1, 58.0, 57.7, 57.4, 55.3, 51.5, 48.5, 47.0, 45.8. HRMS (ESI): calcd for $C_{55}H_{60}BrN_7O_9$ $[M]^{4+}$: 260.3404, found: 260.3409.

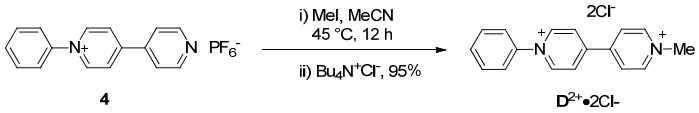

Compound M^{2+}·2Cl⁻. A solution of compound **4**[1] (0.38 g, 1.0 mmol) and methyl iodide (0.36 g, 2.50 mmol) in acetonitrile was stirred at 45 °C for 12 h and then was added tetrabutylammonium chloride (2.78 g, 10.0 mmol). The solution was cooled to room temperature and the formed solid was filtrated. The solid was washed with acetonitrile (50 mL) and dried in vacuo to give compound $\mathbf{M}^{2+}$·2Cl⁻ as a yellow solid (0.30 g, 95%). M.p. 281-283 °C. ^{1}H NMR (400 MHz, D_2O): δ 9.38 (d, *J* = 4.0 Hz, 2H), 9.09 (d, *J* = 8.0 Hz, 2H), 8.71 (d, *J* = 4.0 Hz, 2H), 8.60 (d, *J* = 4.0 Hz, 2H), 7.81-7.77 (m, 5H), 4.52 (s, 3H). ^{13}C NMR (100 MHz, D_2O): δ146.4, 132.0, 130.6, 126.6, 124.0, 48.3. HRMS (ESI): calcd for $C_{17}H_{16}N_2$ $[M]^{2+}$: 124.0651, found: 124.0647.

References

(1) K.-D. Zhang, J. Tian, D. Hanifi, Y. Zhang, A. C.-H. Sue, T.-Y. Zhou, L. Zhang, X. Zhao, Y. Liu and Z.-T. Li, *J. Am. Chem. Soc*., 2013, **135**, 17913.

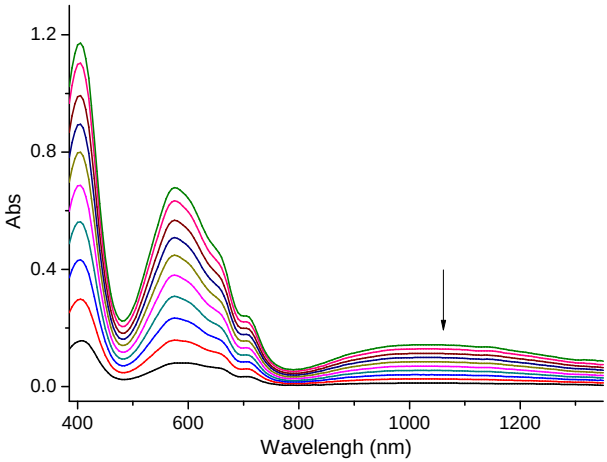

Figure S1. Absorption spectra of $\mathbf{Tr}^{3(\bullet+)}$ from 50 μM to 5 μM in sodium phosphate buffer (0.1 M) containing sodium dithionite (50 mM) at 25 °C.

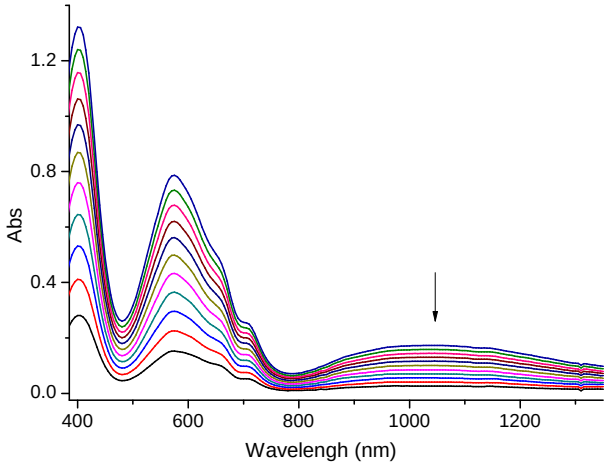

Figure S2. Absorption spectra of $\mathbf{Tr}^{3(\bullet+)}$ from 57 μM to 1.0 μM in sodium phosphate buffer (0.1 M, 7.5% THF) containing sodium dithionite (50 mM) at 25 °C.

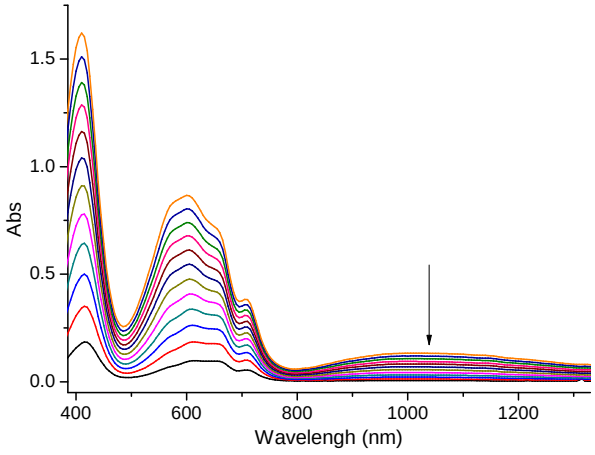

Figure S3. Absorption spectra of $\mathbf{Tr}^{3(\bullet+)}$ from 55 μM to 5.0 μM in sodium phosphate buffer (0.1 M, 15% THF) containing sodium dithionite (50 mM) at 25 °C.

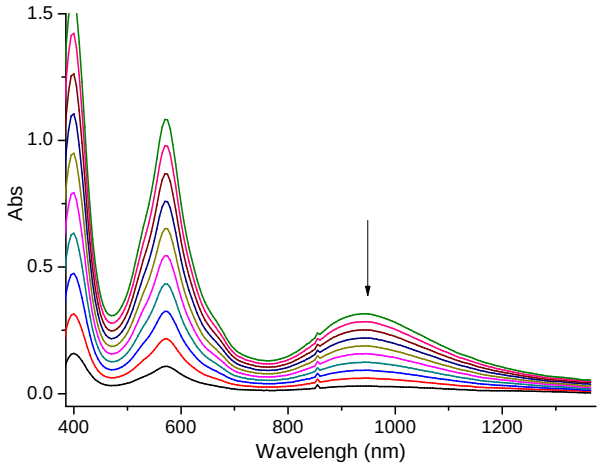

Figure S4. Absorption spectra of $\mathbf{Tr}^{3(\bullet+)}$, in the presence of CB[8] (CB[8] = 1.5 × [$\mathbf{Tr}^{3(\bullet+)}$]), from 47 μM to 5.0 μM in sodium phosphate buffer (0.1 M) containing sodium dithionite (50 mM) at 25 °C.

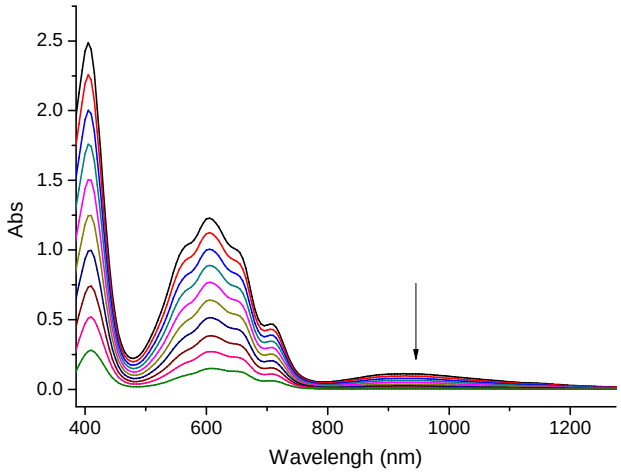

Figure S5. Absorption spectra of $\mathbf{M}^{\bullet+}$ from 95 μM to 5.0 μM in sodium phosphate buffer (0.1 M) containing sodium dithionite (50 mM) at 25 °C.

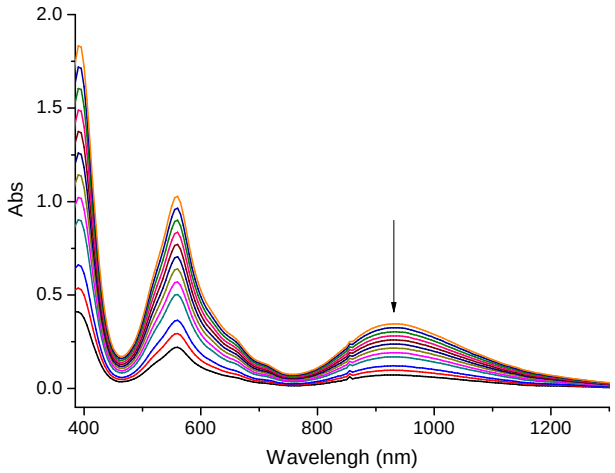

Figure S6. Absorption spectra of $\mathbf{M}^{\bullet+}$, in the presence of CB[8] (CB[8] = 0.5 × [$\mathbf{M}^{\bullet+}$]), from 70 μM to 5.0 μM in sodium phosphate buffer (0.1 M) containing sodium dithionite (50 mM) at 25 °C.

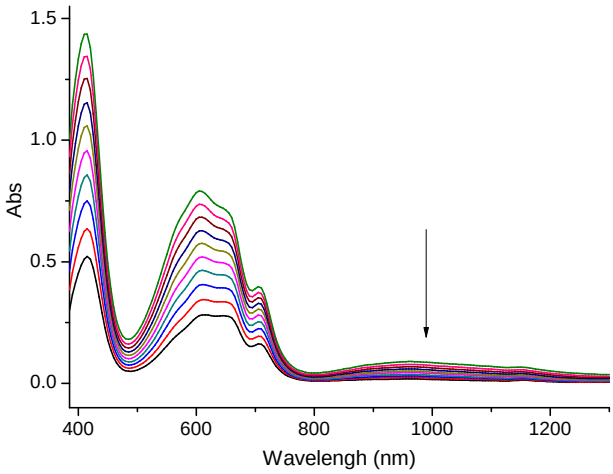

Figure S7. Absorption spectrum of $\mathbf{D}^{2(\bullet+)}$ from 65 μM to 5.0 μM in sodium phosphate buffer (0.1 M) containing sodium dithionite (50 mM) at 25 °C.

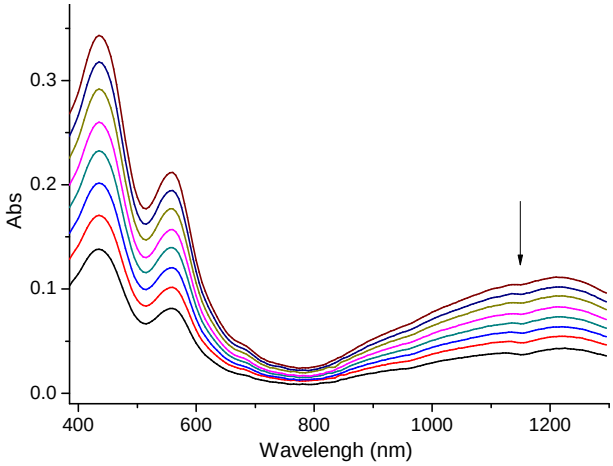

Figure S8. Absorption spectra of $\mathbf{T}^{3(\bullet+)}$ from 40 μM to 4.0 μM in sodium phosphate buffer (0.1 M) containing sodium dithionite (50 mM) at 25 °C.

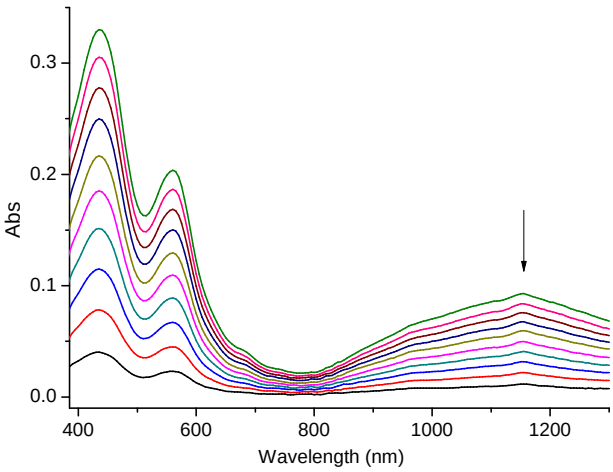

Figure S9. Absorption spectra of $\mathbf{T}^{3(\bullet+)}$ from 40 μM to 1.0 μM in sodium phosphate buffer (0.1 M, 7.5% THF) containing sodium dithionite (50 mM) at 25 °C.

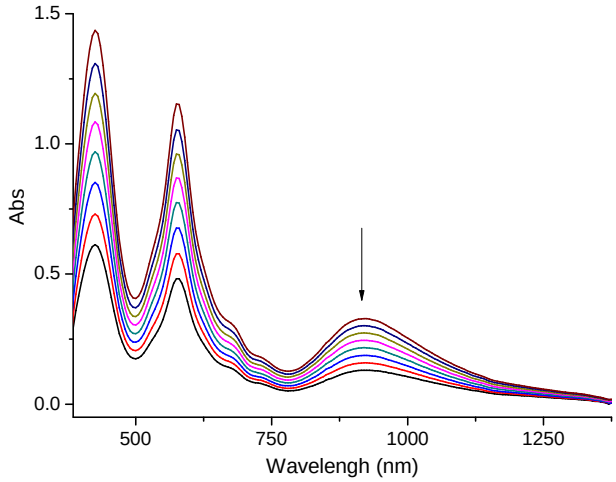

Figure S10. Absorption spectra of $\mathbf{T}^{3(\bullet+)}$, in the presence of CB[8] (CB[8] = 1.5 × [$\mathbf{Tr}^{3(\bullet+)}$]), from 40 μM to 3.0 μM in sodium phosphate buffer (0.1 M) containing sodium dithionite (50 mM) at 25 °C.

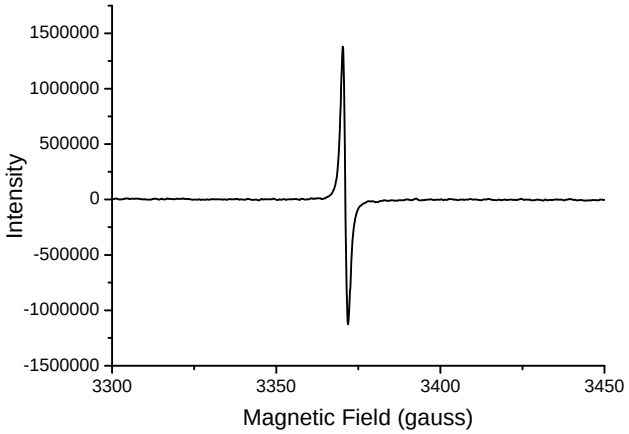

Figure S11. EPR spectrum of $\mathbf{Tr}^{3(\bullet+)}$ (0.033 mM) at 80 °C in sodium phosphate buffer (0.1 M) containing sodium dithionite (50 mM), with the addition of CB[8] (0.05 mM).

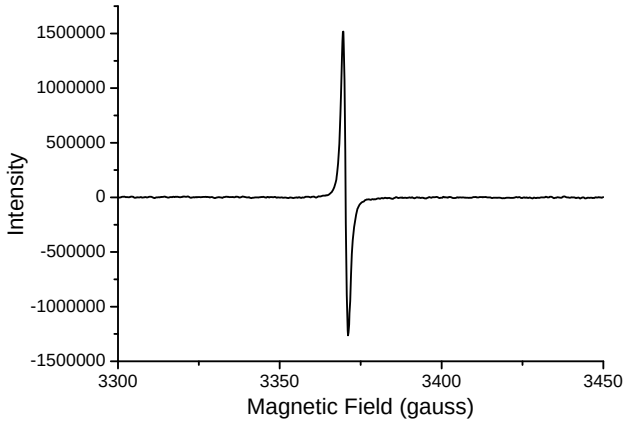

Figure S12. EPR spectrum of $\mathbf{D}^{2(\bullet+)}$ (0.05 mM) at 80 °C in sodium phosphate buffer (0.1 M) containing sodium dithionite (50 mM), with the addition of CB[8] (0.05 mM).

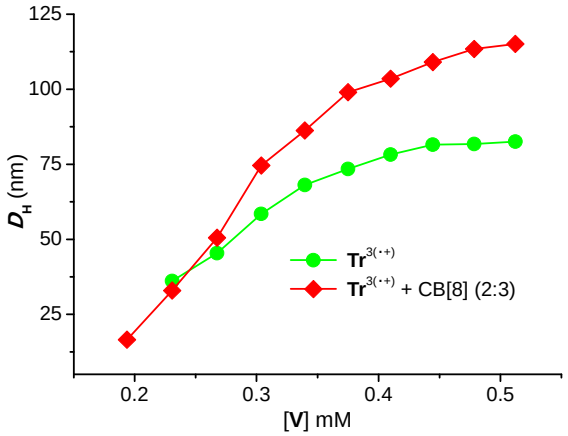

Figure S13. The concentration dependence of D_H of the solution of $\mathbf{Tr}^{3(\bullet+)}$ and its 2:3 mixture with CB[8] in sodium phosphate buffer (0.1 M) in the presence of sodium dithionite (0.05 M) at 25 °C.

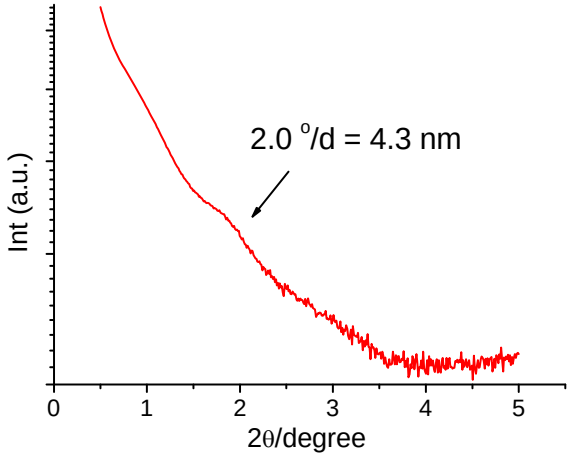

Fig. S14 SAXD profile of the solid sample of $\mathbf{Tr}^{3(\bullet+)}$ obtained by evaporating the aqueous solution of $\mathbf{Tr}^{6+}\cdot 6Cl^-$ (1.0 mM) and CB[8] (1.5 mM) containing sodium dithionite (50 mM).

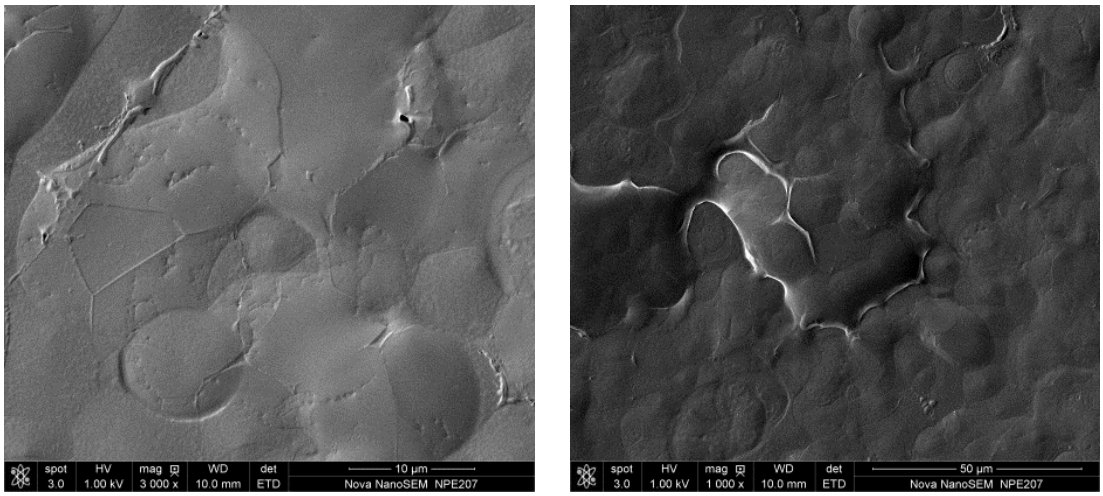

Fig. S15 SEM images of the solid sample obtained by evaporating the aqueous solution of $\mathbf{Tr}^{6+}\cdot 6Cl^-$ (10 µM) containing sodium dithionite (10 mM).

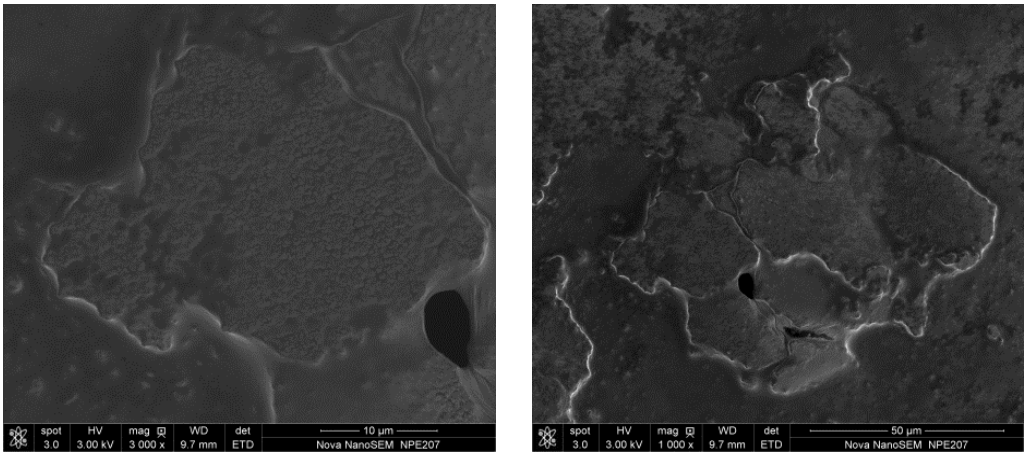

Fig. S16 SEM images of the solid sample obtained by evaporating the aqueous solution of $\mathbf{Tr}^{6+}\cdot 6Cl^-$ (10 μM) and CB[8] (15 μM) containing sodium dithionite (10 mM).

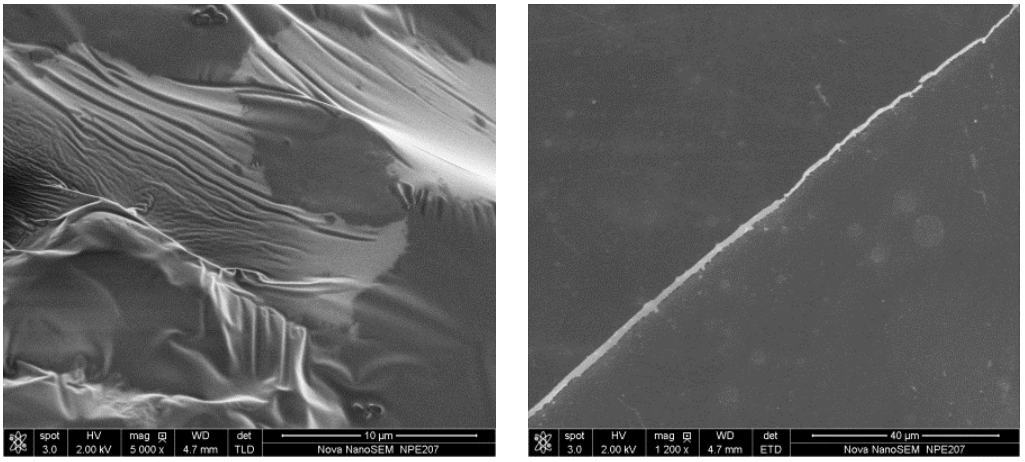

Fig. S17 SEM images of the solid sample obtained by evaporating the aqueous solution of $\mathbf{Tr}^{6+}\cdot 6Cl^-$ (10 μM) after $\mathbf{Tr}^{6+}$ was reduced to $\mathbf{Tr}^{3(\bullet+)}$ with zinc dust.

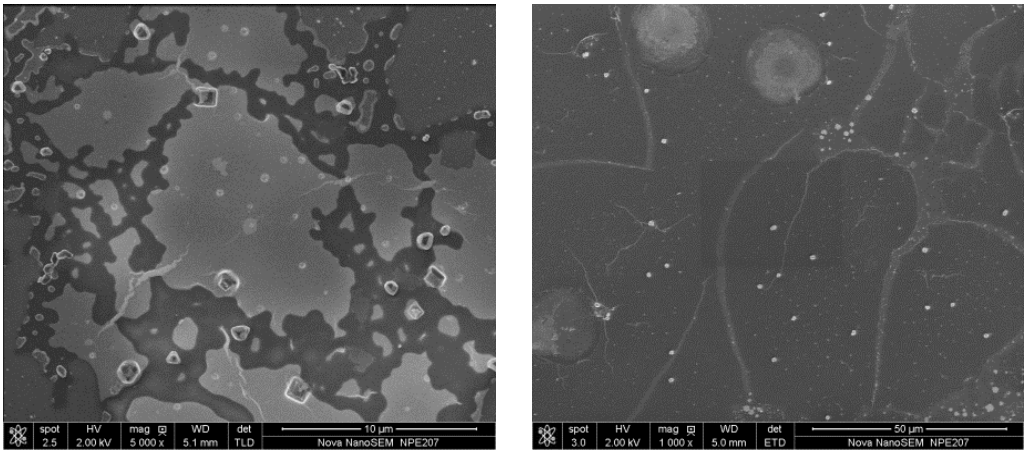

Fig. S18 SEM images of the solid sample obtained by evaporating the aqueous solution of $\mathbf{Tr}^{6+}\cdot 6Cl^-$ (10 μM) and CB[8] (15 μM) after $\mathbf{Tr}^{6+}$ was reduced to $\mathbf{Tr}^{3(\bullet+)}$ with zinc dust.

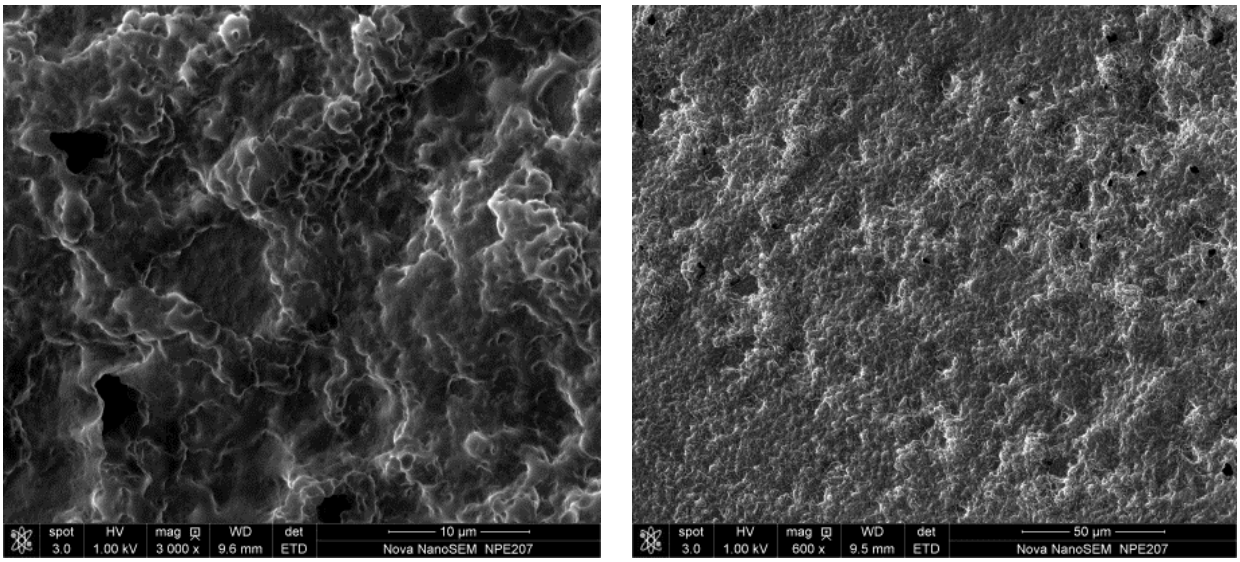

Fig. S19 SEM images of sodium dithionite by evaporating its aqueous solution (10 mM).

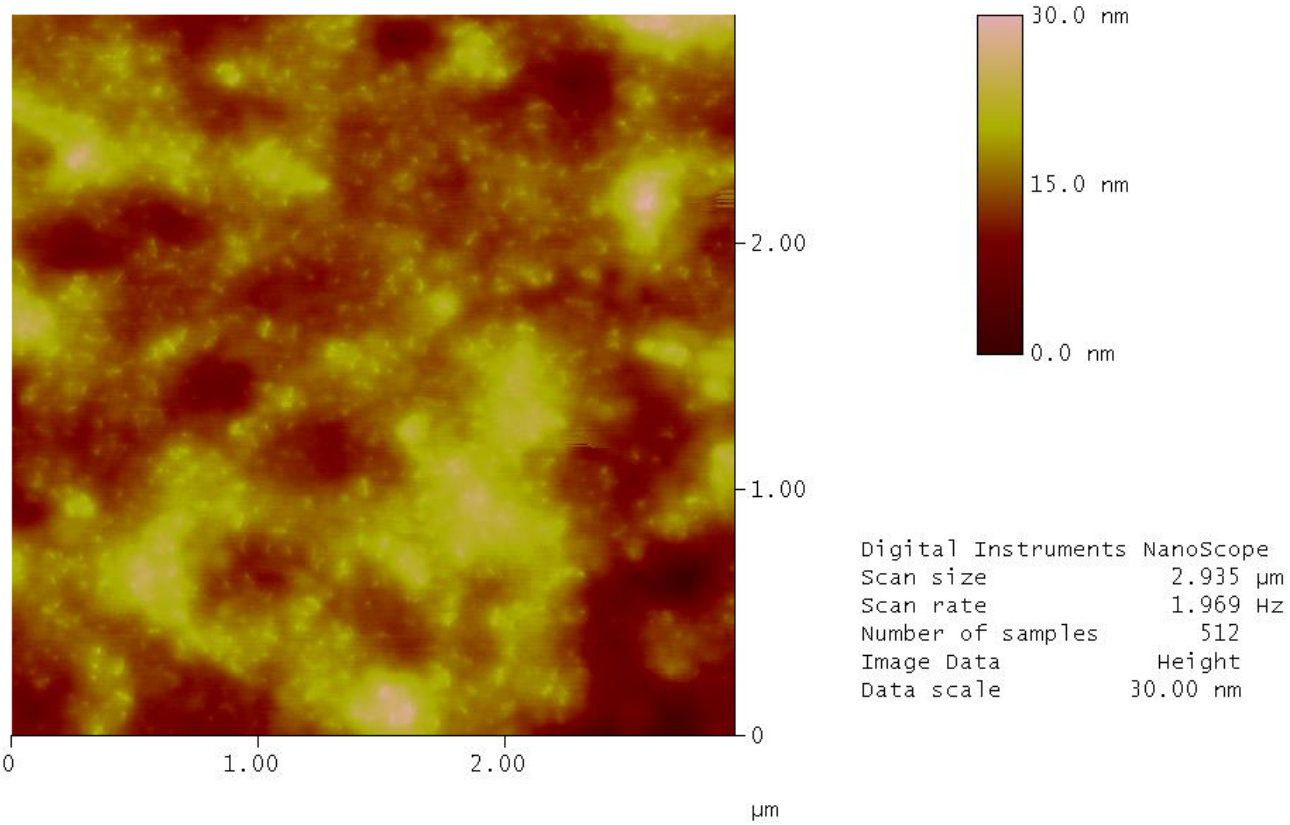

Fig. S20 AFM image of the solid sample obtained by evaporating the aqueous solution of $\mathbf{Tr}^{6+}\cdot 6Cl^{-}$ (10 μM) under reduced pressure after $\mathbf{Tr}^{6+}$ was reduced to $\mathbf{Tr}^{3(\bullet+)}$ with zinc dust.

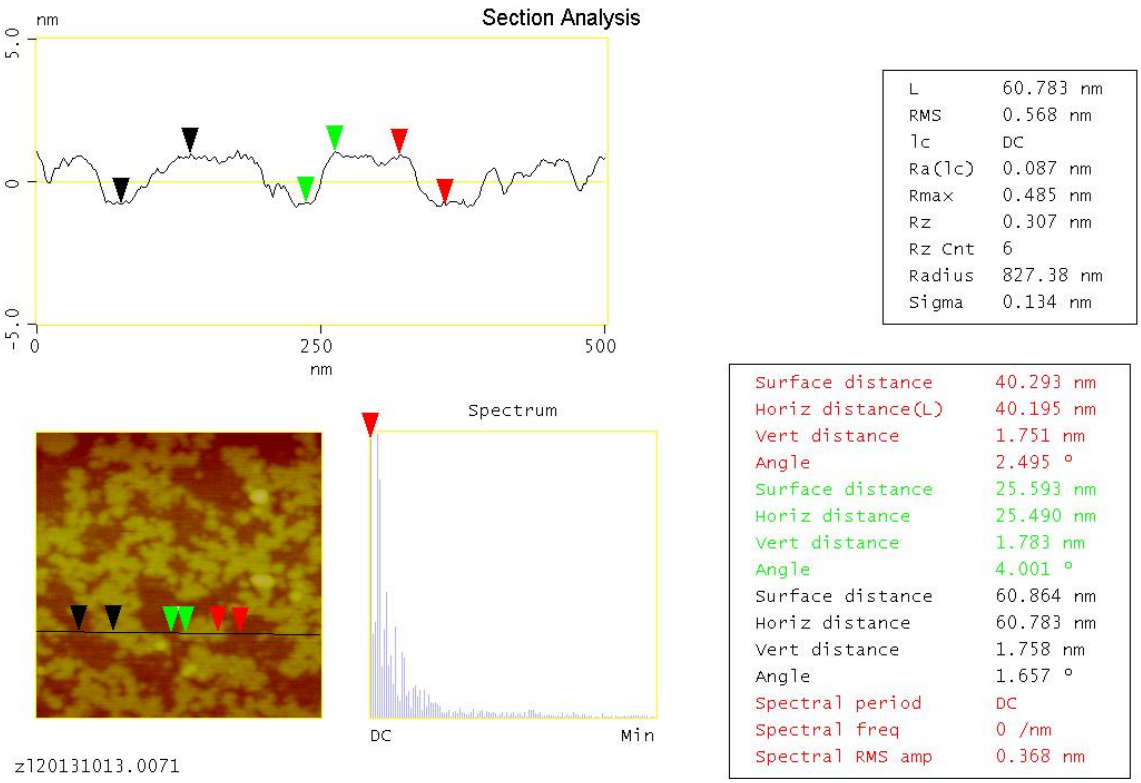

Fig. S21 AFM image of the solid sample obtained by evaporating the aqueous solution of $\mathbf{Tr}^{6+}\cdot 6Cl^{-}$ (10 μM) and CB[8] (15 μM) after $\mathbf{Tr}^{6+}$ was reduced to $\mathbf{Tr}^{3(\bullet+)}$ with zinc dust.

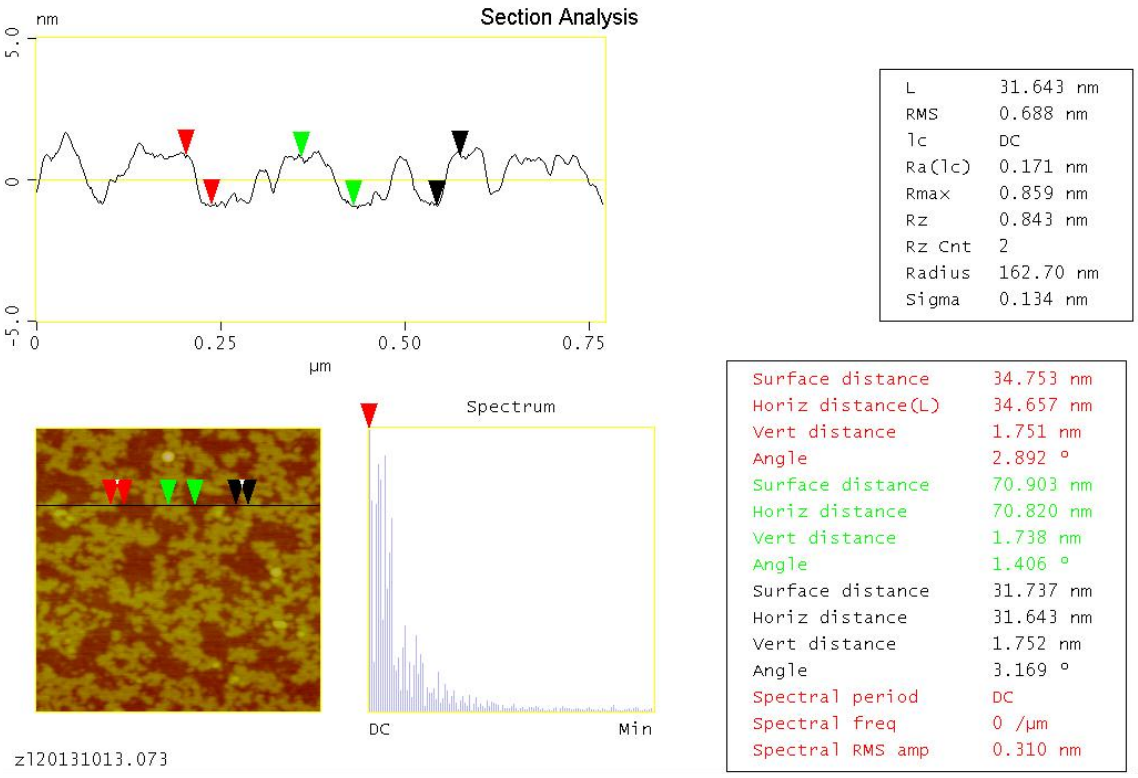

Fig. S22 AFM image of the solid sample obtained by evaporating the aqueous solution of $\mathbf{Tr}^{6+}\cdot 6Cl^{-}$ (10 μM) and CB[8] (15 μM) after $\mathbf{Tr}^{6+}$ was reduced to $\mathbf{Tr}^{3(\bullet+)}$ with zinc dust.

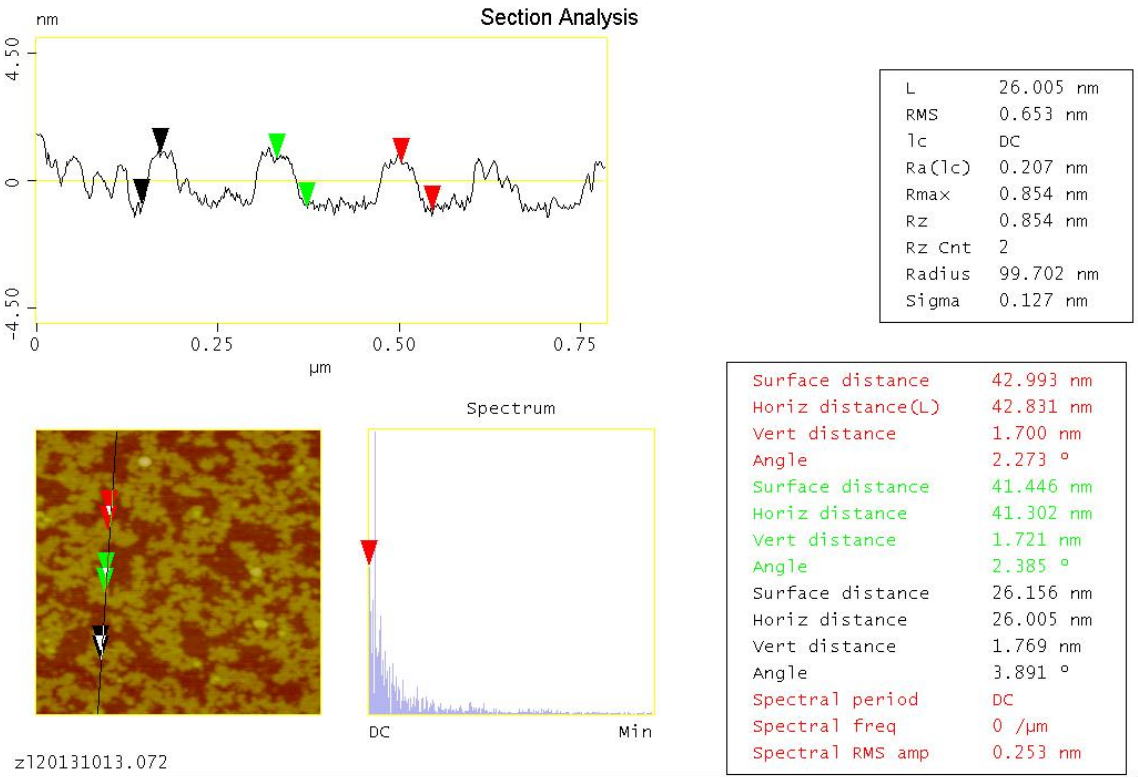

Fig. S23 AFM image of the solid sample obtained by evaporating the aqueous solution of $\mathbf{Tr}^{6+}\cdot 6Cl^{-}$ (10 μM) and CB[8] (15 μM) after $\mathbf{Tr}^{6+}$ was reduced to $\mathbf{Tr}^{3(\bullet+)}$ with zinc dust.

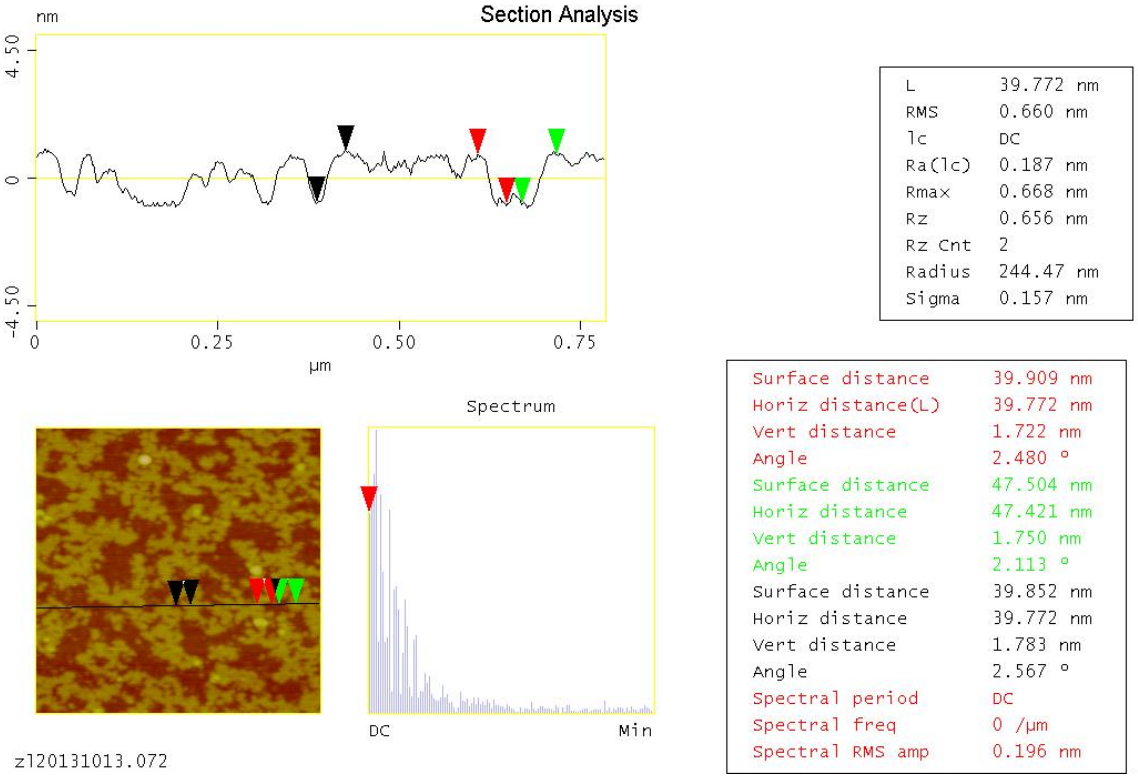

Fig. S24 AFM image of the solid sample obtained by evaporating the aqueous solution of $\mathbf{Tr}^{6+}\cdot 6Cl^{-}$ (10 μM) and CB[8] (15 μM) after $\mathbf{Tr}^{6+}$ was reduced to $\mathbf{Tr}^{3(\bullet+)}$ with zinc dust.

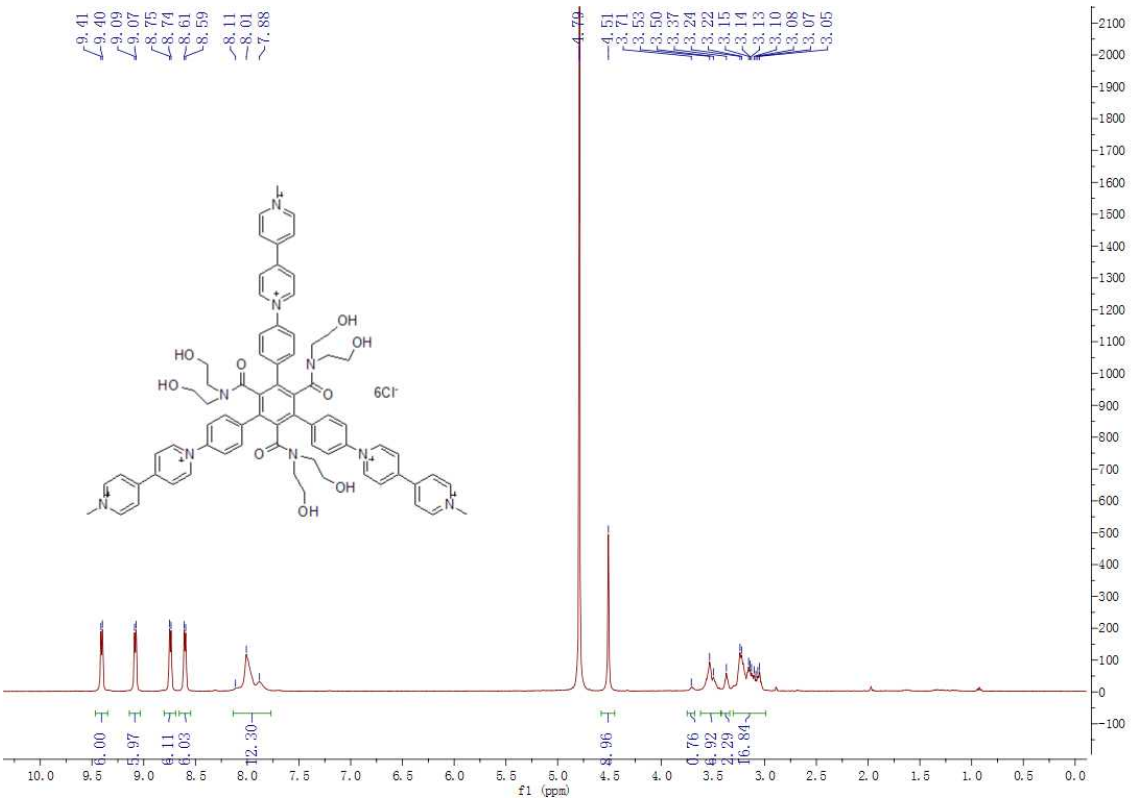

Fig. S25 ^{1}H NMR spectrum (400 MHz) of $\mathbf{Tr}^{6+}\cdot 6Cl^{-}$ in D_2O (0.5 mM).

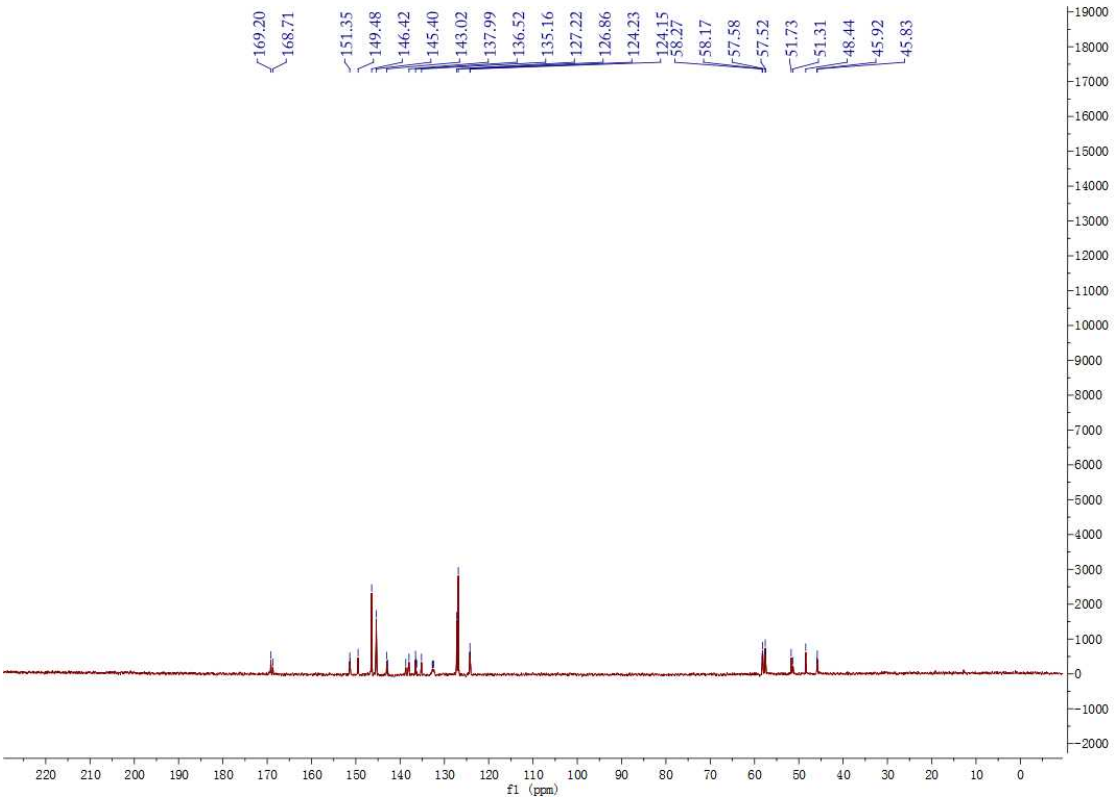

Fig. S26 ^{13}C NMR spectrum (100 MHz) of $\mathbf{Tr}^{6+}\cdot 6Cl^{-}$ in D_2O (10 mM).

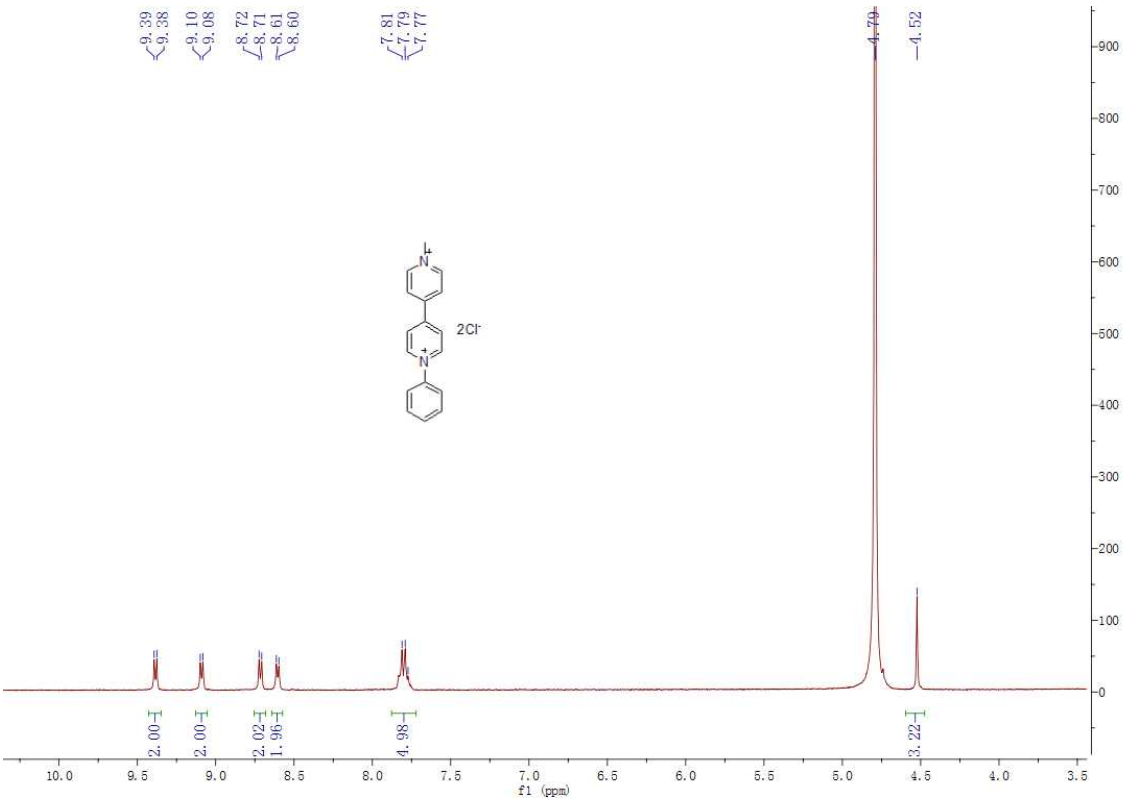

Fig. S27 ^{1}H NMR spectrum (400 MHz) of $\mathbf{M}^{2+}\cdot 2Cl^{-}$ in D_2O (1 mM).

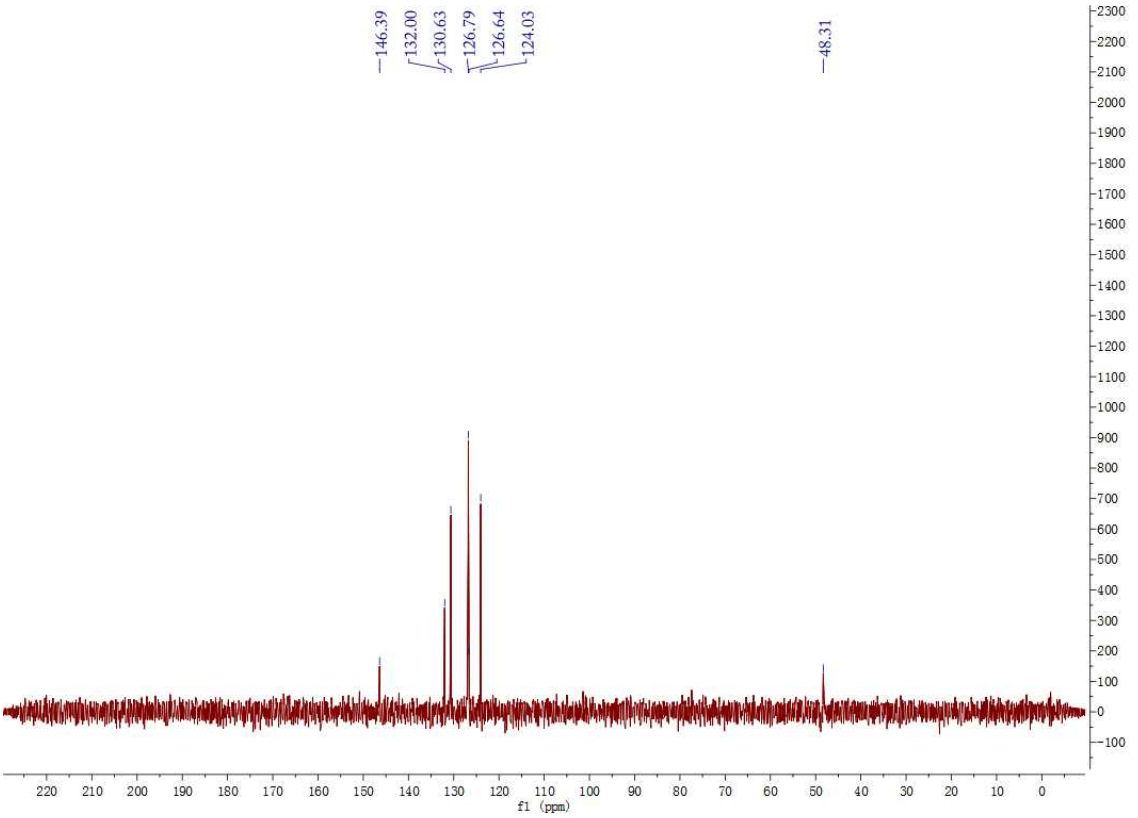

Fig. S28 ^{13}C NMR spectrum (100 MHz) of $\mathbf{M}^{2+}\cdot 2Cl^{-}$ in D_2O (10 mM).

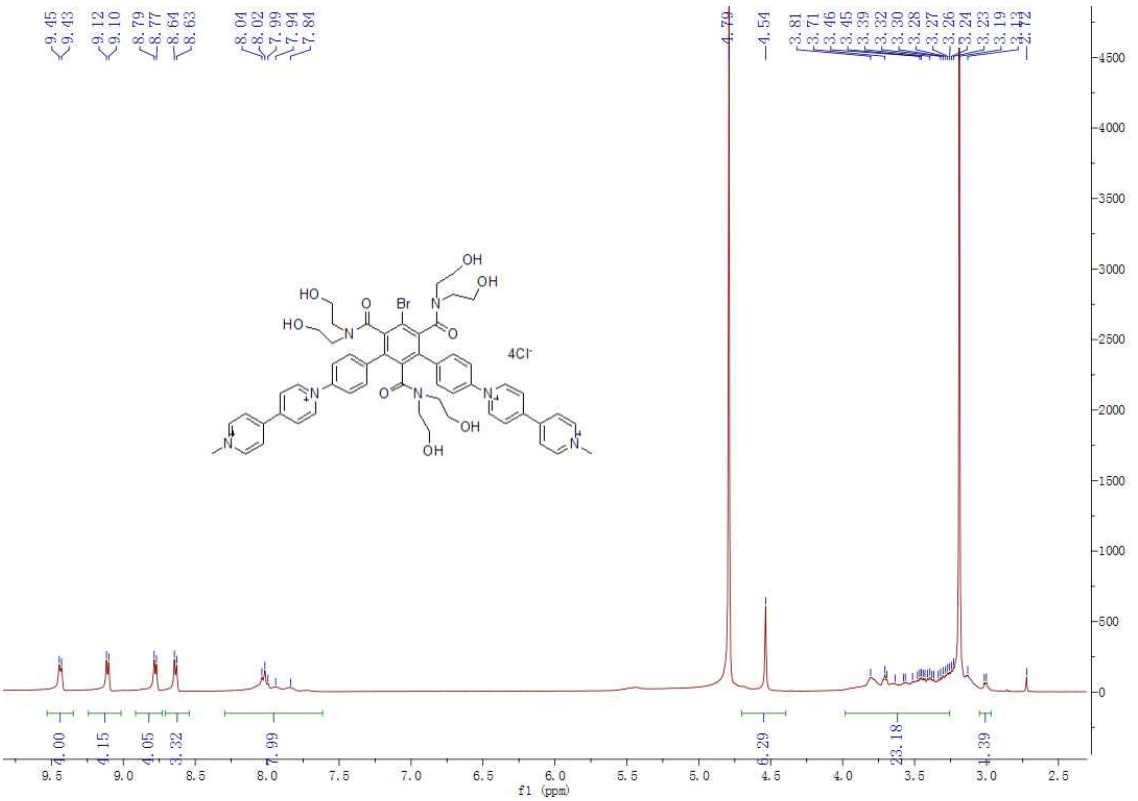

Fig. S29 ^{1}H NMR spectrum (400 MHz) of $\mathbf{D}^{4+}\cdot 4Cl^{-}$ in D_2O (1 mM).

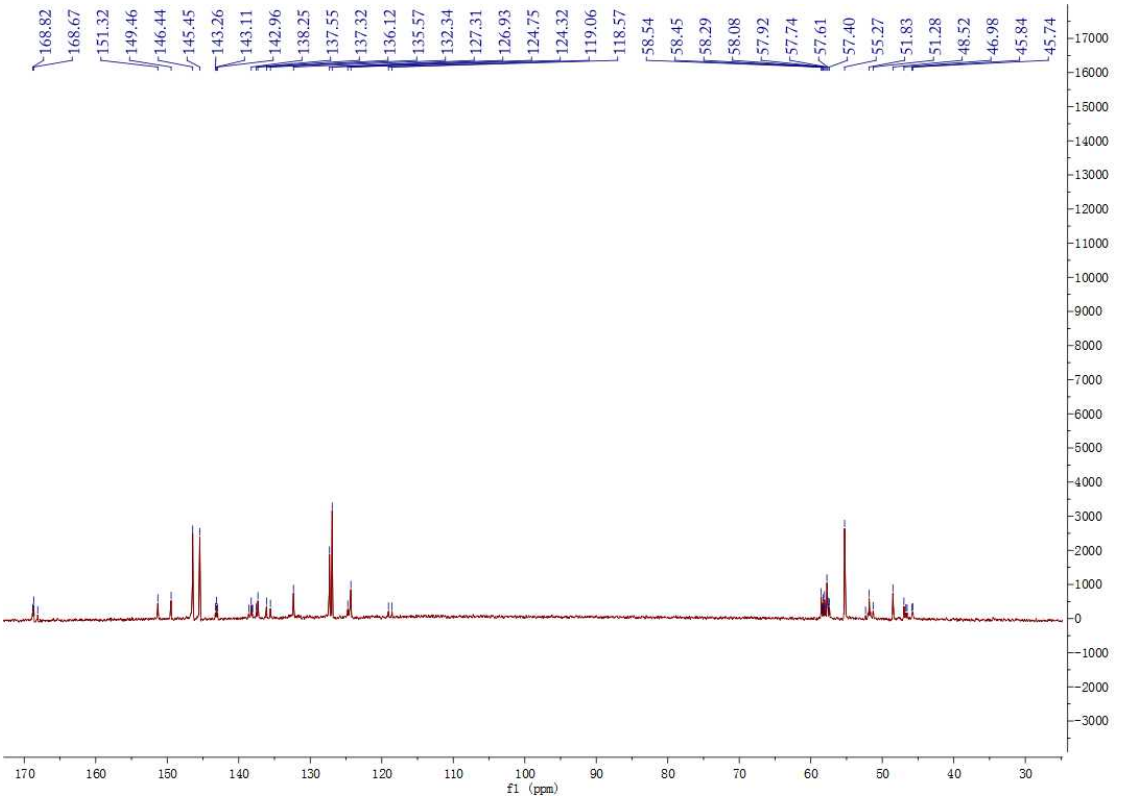

Fig. S30 ^{13}C NMR spectrum (100 MHz) of $\mathbf{D}^{4+}\cdot 4Cl^{-}$ **VsV**4Cl in D_2O (10 mM).

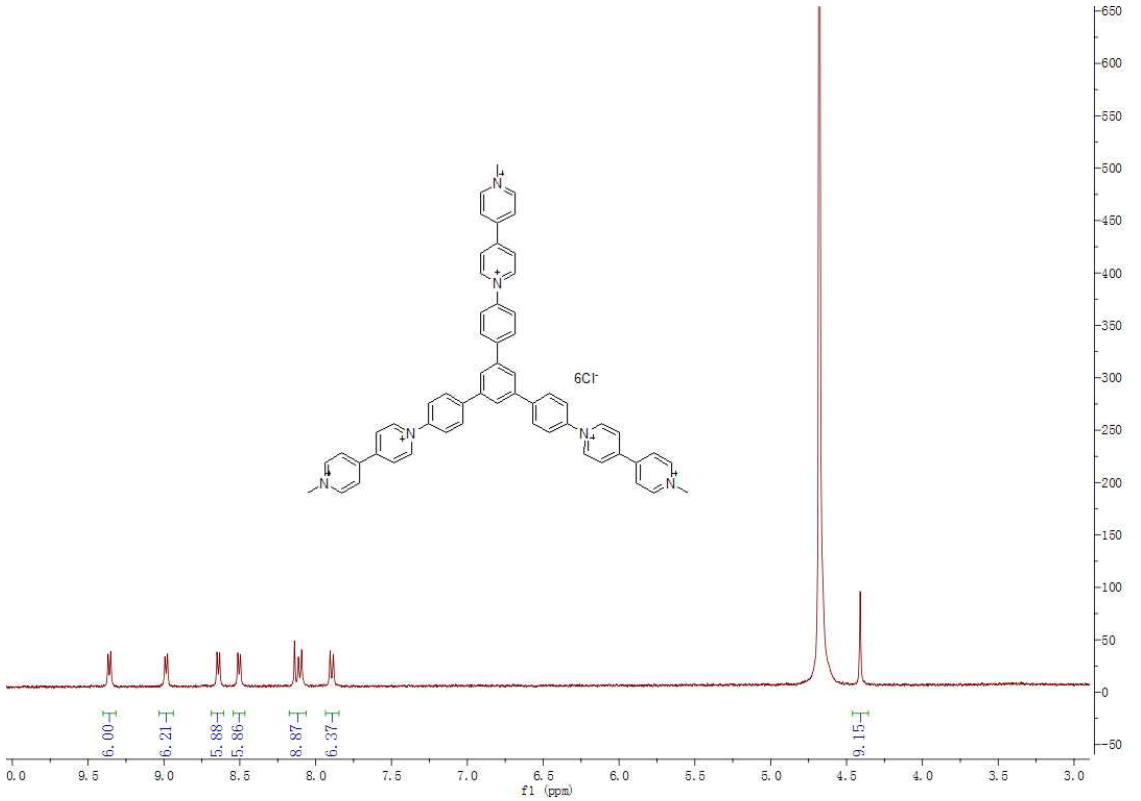

Fig. S31 ^{1}H NMR spectrum (400 MHz) of $\mathbf{T}^{6+}\cdot 6Cl^{-}$ in D_2O (1 mM).

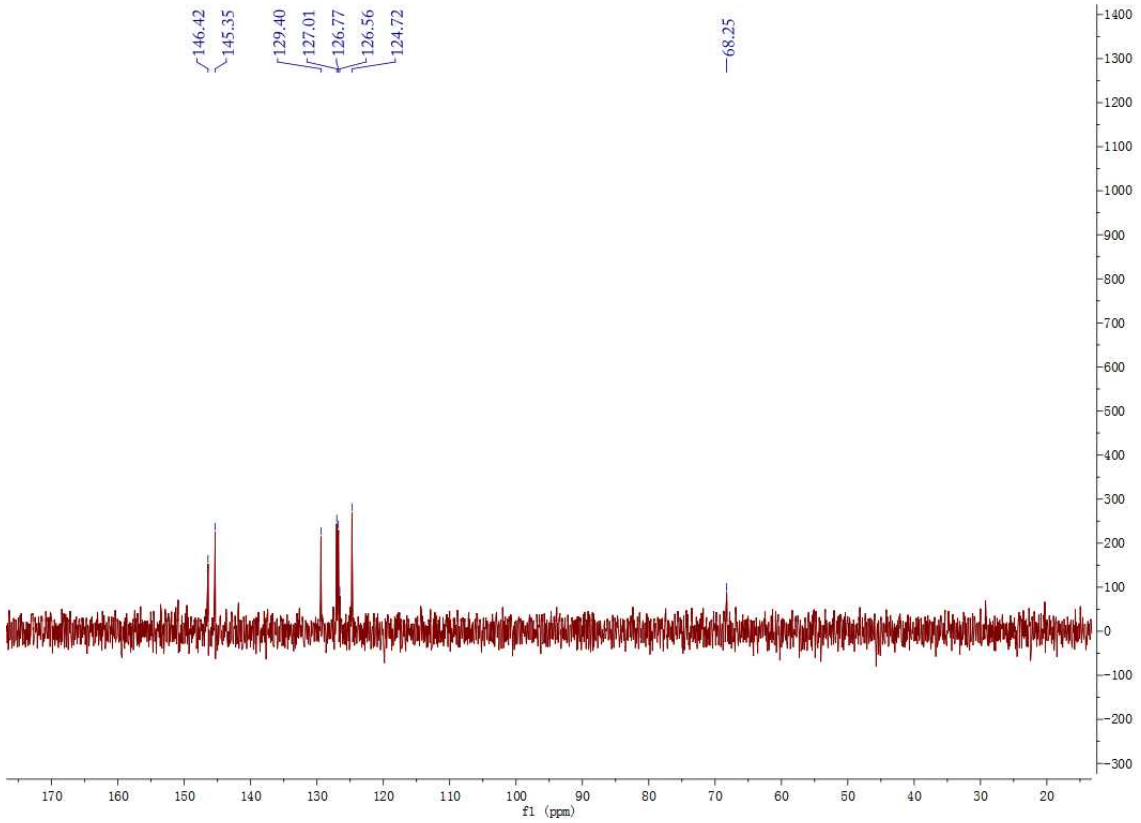

Fig. S32 ^{13}C NMR spectrum (100 MHz) of $\mathbf{T}^{6+}\cdot 6Cl^{-}$ in D_2O (10 mM).